Received: 10 April 2016 | Revised: 14 May 2016 | Accepted: 19 May 2016
DOI: 10.37917/ijeee.12.1.9 | Vol. 12| Issue 1 | June 2016
Open Access
Iraqi Journal for Electrical and Electronic Engineering
Original Article
IJEEE University of Basrh College of Engineering

Numerical Analysis of Thermal Dependence of the Spectral Response of Polymer Optical Fiber Bragg Gratings

Hisham K. Hisham
Department of Electrical Engineering, Faculty of Engineering,
Basra University
Basra, Iraq
E-mail: husham_kadhum@yahoo.com.

Abstract
The thermal dependence of the spectral response (i.e. transmission, reflection and time delay (τ_r) responses) of uniform polymer optical fiber (POF) Bragg gratings has been investigated. In addition to the temperature dependence, the effects of grating strength (kL_g) and fiber index modulation (Δn) have been investigated. Besides high capability of tunable wavelength due to the unique large and negative thermo-optic coefficient of POF, the spectral response for POF Bragg gratings show high stability and larger spectrum bandwidth with temperature variation compare with the silica optical fiber (SOF) Bragg gratings, especially with the increase of the kL_g value. It was found that by increasing kL_g, the peak reflectance value increases and the bandwidth of the Bragg reflector become narrower. Also it's shown by increasing the kL_g value, τ_r deceasing significantly and reach its minimum value at the designed wavelength (λ_B). Furthermore, the τ_r for POF Bragg gratings is less than that for SOF Bragg gratings at the same value of kL_g. Also it's found that the peak reflectivity value increases to around 60% when the Δn value increases from $1{\times}10^{-4}$ to $5{\times}10^{-4}$.

Index Terms—**Fiber Bragg gratings (FBGs), polymer optical fiber (POF) Bragg gratings, temperature effect, spectral response.**

I. INTRODUCTION

One of the most significant development in the field of optical engineering over the last three decades has been the emergence of the fiber Bragg grating (FBG), which has the found major applications in telecommunications and sensor systems [1]. With the development of wavelength division multiplexed-passive optical network (WDM-PON) system for broad-band, network-security, and high-speed transmitted data capacity, FBGs have become indispensable elements in optical communications systems due to its unique features such as wavelength selectivity, high tunability, and low-loss characteristics [2, 3].

In addition to use FBGs as reflectors, wavelength tuning and fiber sensing are the two major applications for gratings fiber [4]. In these applications, the FBG is controlled by an external environment such as temperature [5-7]. The sensitivity of the Bragg wavelength to temperature arises from the change in period associated with the thermal expansion of the fiber coupled with a change in the refractive index arising from the thermo-optic [8-10].

However, for silica optical fiber (SOF) Bragg gratings, the thermal tunability is the problem, where the change in the Bragg wavelength due to the changes in temperature is very small, which are not meet the requirements for WDM systems since the expected bandwidth of these systems in the future will be more than 100 nm [10–12]. This is because the SOF Bragg grating has small thermal effect and large Young's modulus [13]. Though the range of the wavelength tunability can be increased by the compression [14], but the reproducibility and reversibility is very low [9]. Moreover, to satisfy this we need a complicated and bulky components lead to increase in the system cost [15-18].

In the case of polymer optical fiber (POF) Bragg gratings, the situation is totally different because the thermal effect is much more than those of SOF Bragg gratings [14]. For example, the Young's modulus for the polymer is (0.1 x 1010 N/m2) compare with (7.13 x 1010 N/m2) for silica, is more than 70 times smaller [13, 14], that make the tunability is much better than that of SOF Bragg gratings. In addition, POF Bragg grating has the merits of a negative and large thermo-optic effect, thereby, large refractive index tuning by heating can be obtained higher than for SOF Bragg gratings [15- 16]. Consequently, high tuning range can be obtained easily by direct heating for POF Bragg gratings. Furthermore, the flexibility of the POF Bragg gratings can make the tunability extend beyond the thermo-optic effect limitation [20–28].

Because of the plurality promising applications for the POF Bragg gratings in optical communication systems and sensing fields, the temperature effect on its spectra response (i.e. transmission, reflection and time delay responses) is very important, attractive and indispensable to study. In this paper, the thermal dependence of the spectral response of POF Bragg gratings with uniform index change has been investigated for the first time, based on our best knowledge. The paper is structured as follows: The theory for the spectral response of fiber Bragg grating is given in Section 2. The simulation results are discussed in Section 3 followed by the conclusions.

II. Fiber Bragg Gratings Spectral Response

Fiber Bragg gratings (FBGs) are in-fiber gratings operate by acting as a wavelength dependent stop-band filter formed by introducing a periodic perturbation of the effective refraction index within the core of an optical fiber [12]. Two important parameters characterize FBGs, namely, the modulation function of the fiber effective refractive index, n_{eff} and the length of the grating, Λ. Any change in the n_{eff} or Λ of the fiber will result in a Bragg wavelength shift [12, 18]. In the case of uniform FBGs, Λ stay constant throughout the total grating length, L_g and the reflected light is maximum at the Bragg wavelength λ_B, which is given by [12, 18]

$$\lambda_B = 2n_{eff}\Lambda \qquad (1)$$

As we mentioned in the pervious section, in POF Bragg grating, n_{eff} can be change by many mechanisms such as ablation, bond breaking, photo-polymerization, cross-linking, and photo-isomerization [18]. Independent to the mechanism that used, the change in n_{eff} is proportional to the time of exposure and to the ultraviolet intensity [18].

Since n_{eff} is temperature dependent, thus any change in the temperature will result in Bragg wavelength shifts. Based on (1), the shifts in the λ_B of a FBG due to the temperature change is given by [12]

$$\Delta\lambda_B = 2\left(\Lambda\frac{\partial n_{eff}}{\partial T} + n_{eff}\frac{\partial \Lambda}{\partial T}\right)\Delta T \qquad (2)$$

Replacement of $\frac{\partial n_{eff}}{\partial T} = \xi n_{eff}$, where ξ is the thermo-optic coefficient of the fiber core, $\frac{\partial \Lambda}{\partial T} = \alpha\Lambda$, where α is the thermal expansion coefficient of the fiber material, and ΔT is the temperature change gives

$$\frac{\Delta\lambda_B}{\lambda_B} = (\xi + \alpha)\Delta T \qquad (3)$$

The effective refractive index variation of the Bragg grating is given as [129]

$$n_{eff}(z) = n_{eff} + \Delta n_{eff}(z)\left[1 + m\cos\left(\frac{2\pi}{\Lambda}z\right)\right] \qquad (4)$$

where Δn_{eff} (z) is the "dc" index change spatially over a grating period, and *m* represent the grating modulation index. Coupled-mode theory has been used as a powerful tool to describe the optical prosperities of most gratings. The inter-coupling between forward propagation field *A(z)* and backward propagation field *B(z)* can be written as [18]

$$\frac{dA}{dz} = i\left(\delta + \frac{2k_c}{m} - \frac{1}{2}\frac{d\phi}{dz}\right)A(z) + ik_c B(z) \qquad (5)$$

$$\frac{dB}{dz} = -i\left(\delta + \frac{2k_c}{m} - \frac{1}{2}\frac{d\phi}{dz}\right)B(z) - ik_c^* A(z) \qquad (6)$$

where the amplitudes *A* and *B* are defined as $A(z) = A(z).\exp(i\delta z - \phi/2)$, $B(z) = B(z).\exp(-i\delta z + \phi/2)$. In these equations, k_c is the coupling coefficient between forward and backward waves, δ is the deviation of propagation constant β from the Bragg condition, which is independed of z for all FGs, is given as [12]

$$\begin{aligned}\delta &= \beta - \beta_o \\ &= \beta - \frac{\pi}{\Lambda} \\ &= 2n_{eff}\left(\frac{1}{\lambda} - \frac{1}{\lambda_B}\right)\end{aligned} \qquad (7)$$

Finally, the factor $(1/2)d\phi/dz$ represents the chirp of the grating period. The term inside the parenthesis in (5) and (6) is the dc self-coupling coefficient, and is given by $\hat{\sigma} = (\delta + 2k_c/m - d\phi/2dz)$ [36]. For single-mode Bragg grating reflector with sinusoidal variation of effective index change along the fiber axis, we can use the simple relation for the coupling coefficient k_c [12]

$$k_c = k_c^* = \frac{\pi}{\lambda_B}\left(\Gamma\Delta n_{eff}\right) \qquad (8)$$

where Γ is the fraction of the fiber mode power that contained in the gratings fiber. For uniform Bragg grating along fiber axis, Δn_{eff} and k_c are constants, and $d\phi/dz = 0$. Thus, (5) and (6) are coupled first order-ordinary differential equations with constant coefficients, for which a closed-form solution for a uniform FBGs of length L_g can be found by assuming that $A(-L_g/2)$ and $B(L_g/2)$. Depending to the schematic diagram shown in Figure 1, the relations of the A and B at the two ends of grating fiber can given as

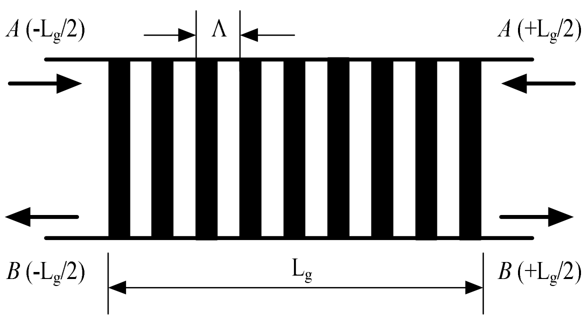

Figure 1 Uniform fiber Bragg gratings

$$\begin{bmatrix} A(-L_g/2) \\ B(-L_g/2) \end{bmatrix} = \begin{bmatrix} \psi & \varsigma \\ \varsigma^* & \psi^* \end{bmatrix} \times \begin{bmatrix} A(L_g/2) \\ B(L_g/2) \end{bmatrix}$$

$$= \begin{bmatrix} \cos(\Omega L_g) - i\frac{\zeta}{\Omega}\sin(\Omega L_g) & -i\frac{k_c}{\Omega}\sin(\Omega L_g) \\ i\frac{k_c}{\Omega}\sin(\Omega L_g) & \cos(\Omega L_g) + i\frac{\zeta}{\Omega}\sin(\Omega L_g) \end{bmatrix} \times \begin{bmatrix} A(L_g/2) \\ B(L_g/2) \end{bmatrix} \quad (9)$$

Then, the amplitude reflection coefficient $\rho = B(-L_g/2)/A(-L_g/2)$ can be obtain by imposing the boundary conditions as

$$\rho = \frac{ik_c \sin(\Omega . L_g)}{\Omega \cos(\Omega . L_g) - i\zeta \sin(\Omega . L_g)} \quad (10)$$

Where $\Omega = \sqrt{k_c^2 - \zeta^2}$. The power reflection coefficient R of the grating fiber is equal to the square of the magnitude of the complex amplitude reflection coefficient given in (10). Moreover, the first derivative of the Bragg grating reflection coefficient phase φ_r with respect to the frequency ω is identified as a time delay τ_r for the light reflected off of a grating. Thus, τ_r is given as [29, 36]

$$\tau_r = \frac{d\varphi_r}{d\omega} = -\frac{\lambda^2}{2\pi c}\frac{d\varphi_r}{d\lambda} \quad (11)$$

In (11), c is the speed of light in vacuum.

III. RESULTS AND DISCUSSION

Figure 2 (a) and (b) shows the wavelength dependence of the transmission and reflection spectra response for three different values of kL_g for SOF-POF Bragg gratings at room temperature, respectively. The reflection and transmission peak values are obtained by adjusting k_c in equations (5) and (6). As shown, the reflectivity is maximum at the designed wavelength (λ_B) and by increasing the kL_g value, the peak reflectance will increase due to increase the reflection light from the grating plants and the bandwidth of the Bragg reflector (i.e. the width between the first zeros on either side of the maximum reflectivity [12]) becomes narrower. This indicates that the bandwidth of the grating reflector can be tuned to a desired value by varying the kL_g value. Also, results observe that for the same value of kL_g, the bandwidth for SOF Bragg gratings is narrower with lower reflectivity than that for the POF Bragg gratings.

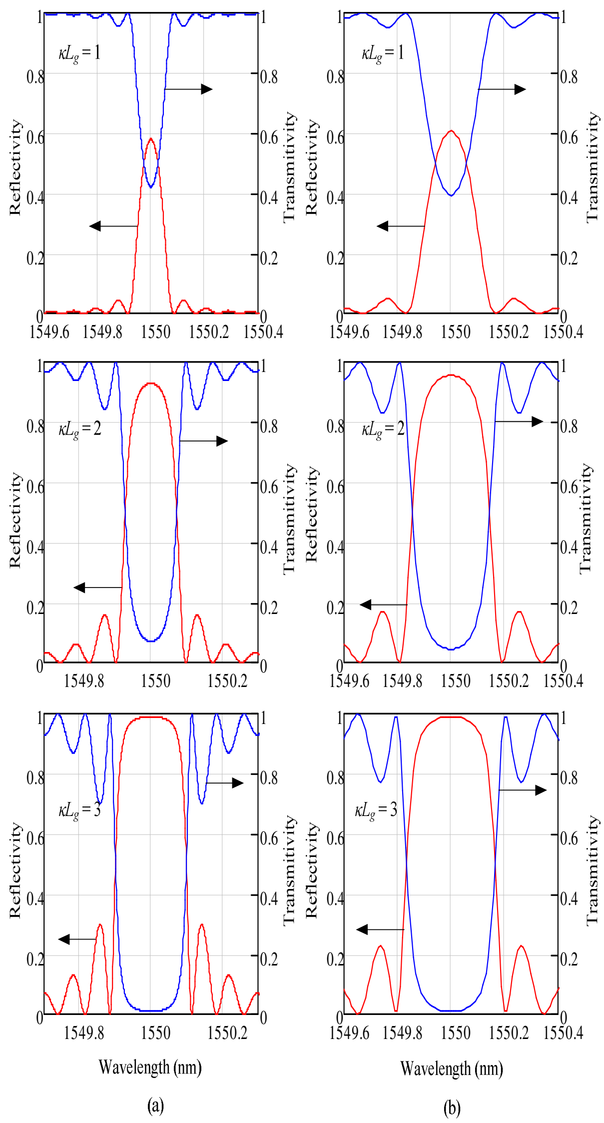

Figure 2 Reflection (red curves) and transmission (blue curves) spectral response versus wavelength for (a) SOF Bragg gratings and (b) POF Bragg gratings, respectively.

Figure 3 (a) and (b) shows the reflectivity and time delay, τ_r responses for three different values of kL_g for SOF-POF Bragg gratings at room temperature, respectively. Clearly, both reflectivity and τ_r are symmetrical about the designed wavelength (λ_B). As shown, by increasing the kL_g value, τ_r deceasing significantly due to reduce the rate change in the phase of the reflected light and reach its minimum value at the λ_B for both SOF and POF. In addition, τ_r becomes appreciable near the band edges and side lobes of the reflection spectrum, where it tends to vary rapidly with wavelength. Also, results shown that the τ_r for POF Bragg gratings is less than that for SOF Bragg gratings at the same value of kL_g. For example, when kL_g = 1, the τ_r at the λ_B for POF Bragg gratings is 18.7 ps compare with 73.6 ps for SOF Bragg gratings. Furthermore, when kL_g increases to 3, the τ_r for POF Bragg gratings decreases to 10.1 ps compare with 32 ps for SOF Bragg gratings. This means that, for the same value for kL_g, the rate change in the phase of the reflected light in the POF Bragg gratings is less than that for the SOF Bragg gratings.

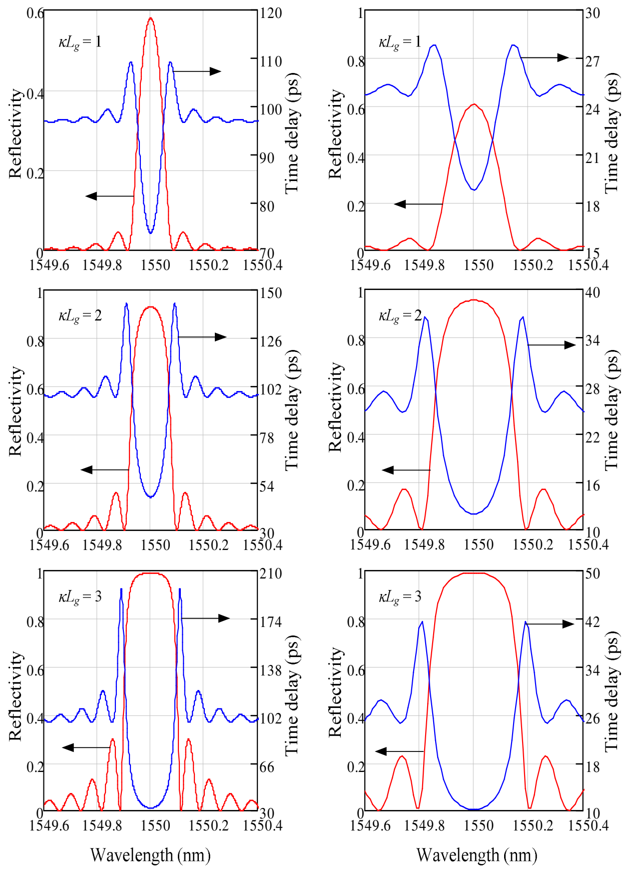

(a) (b)

Figure 3 Reflections (red curves) and delay time (blue curves) spectral response versus wavelength for (a) SOF Bragg gratings and (b) POF Bragg gratings, respectively.

Figure 4 (a) and (b) shows the effect of temperature variation on the reflection (red curves) and transmission (blue curves) spectral response for SOF-POF Bragg gratings for different values of kL_g, respectively. In this study, the temperature effect on the spectral response of a uniform Bragg grating reflector is investigated according to its effect on the effective refractive index of the fiber. The temperature dependent of the fiber refractive index is defined as [6]

$$X(T) = X_O + \frac{\partial X}{\partial T}(T - T_O) \quad (12)$$

where X_o is the initial value found at the reference temperature (T_o), which in this study is considered at the room temperature (T_o = 25 ºC). As shown, the reflection and transmission spectra responses are symmetric around T_o and the peak value of the reflectivity occurs at T_o. This result is consistent with (12). In addition, the reflectivity of SOF Bragg gratings with kL_g = 1 is decreases significantly from 58% to 0.05% by changing temperature ΔT = 10° C (from 25 to 35°C). In contrast, by changing temperature ΔT = 50° C (from 25 to 75°C), the reflectivity of POF Bragg gratings decrease from 60% to 15%. While, by increasing the kL_g from 1 to 3, the SOF reflectivity reduces from 99% to 6.5% comparing with the reduction in the POF reflectivity from 99% to 89%.This results is consistent with that given in Figure 2 about the effect of kL_g. In addition, Figure 4 shows that the POF Bragg gratings have high stability with temperature compare with that for SOF Bragg gratings. This preference for POF Bragg gratings is due to the negative and large thermo-optic coefficient compare with that for SOF. Furthermore, Figure 4 shows the superiority of high temperature tunable POF Bragg gratings against the SOF Bragg gratings. Moreover, the spectrum bandwidth of the POF Bragg gratings is larger than that for the SOF Bragg gratings with temperature variation, especially with the increase of the kL_g, where by increasing kL_g from 1 to 3, the range of temperature operation for the first zero of the reflection spectral is increase.

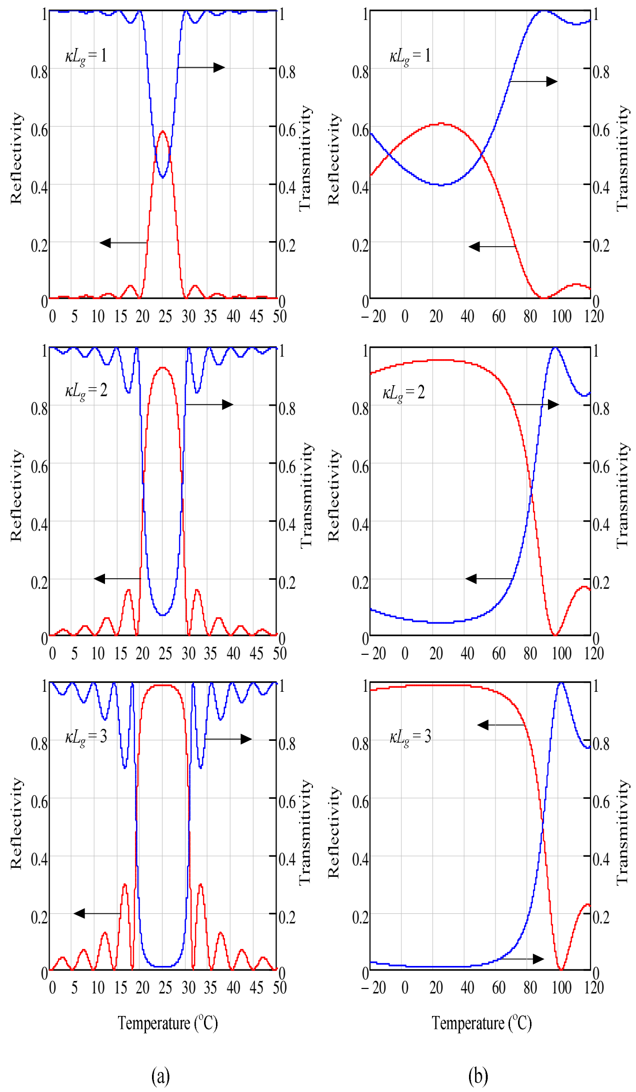

Figure 4 Reflection (red curves) and transmission (blue curves) spectral response verses temperature variation for (a) SOF Bragg gratings, and (b) POF Bragg gratings, respectively.

Figure 5 (a) and (b) shows the effect of temperature variation on the reflectivity and delay time (τ_r) spectral response for SOF-POF Bragg gratings for different values of kL_g, respectively Based on (12), the minimum value of the τ_r is occurs at the reference temperature T_o, where the reflectivity is maximum and the change in the phase for the reflected light is at the minimum value. In addition, the temperature operation range for low τ_r in POF Bragg gratings is greater than that for SOF Bragg gratings.

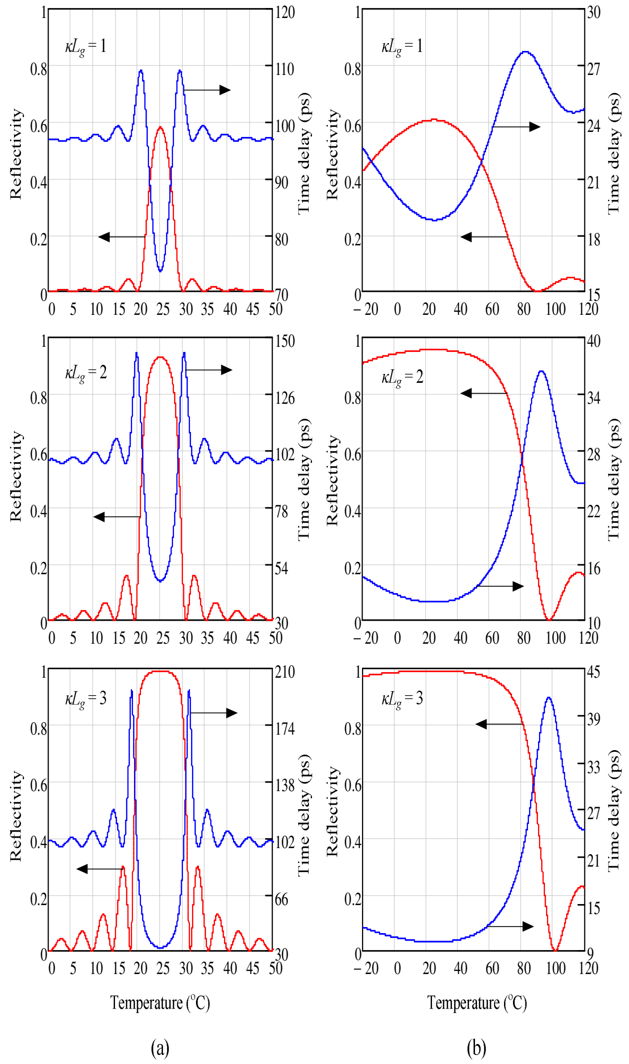

Figure 5 Reflection (red curves) and delay time (blue curves) spectral response verses temperature variation for (a) SOF Bragg gratings, and (b) POF Bragg gratings, respectively.

Figures 6 and 7 shows the effect of temperature variation on the spectral response for SOF-POF Bragg gratings for two different values of the fiber index modulation (Δn), respectively. Although the range of temperature operation is large for the grating length (L_g) is equal to 1 mm as shown in Figure 6, however; the peak value of the reflectivity is very low; where is around 4%. In contrast, the peak reflectivity value increases to around 60% when the Δn value increases to $5{\times}10^{-4}$ as shown in Figure 7 due to induced the refractive index of the core of the optical fiber as given in (4) which leads to increase the cumulative interference between the reflected light. In addition, the grating bandwidth is length limited (the case of weak grating; i. e. the index of refraction change is weak), specifically more for the SOF Bragg gratings. in other words the bandwidth of weak grating is limited by their length, where with the increase of the L_g, the grating bandwidth is change. In contrast, when the L_g increases to 5 mm and 10 mm with Δn value equal to $5{\times}10^{-4}$, the SOF Bragg gratings bandwidth becomes length independent (i. e. strong grating). This mean that the bandwidth is similar wether measured at the band edges, at the first zeros or as the full width half maximum.

Finally, Figures 8 and 9 shows the effect of temperature variation on the time delay (τ_r) spectra for SOF-POF Bragg gratings with Δn equal to $1{\times}10^{-4}$ and $5{\times}10^{-4}$, respectively. It is observed that for $1{\times}10^{-4}$ index modulation, by increasing the L_g from 1 mm to 10 mm, the peak τ_r increasing. In contrast, for $5{\times}10^{-4}$ index modulation, the increasing in the peak value of the τ_r with L_g is reduced. It is clear from the results that given in Figures 6–9, the temperature operation range for high reflectivity and lower time delay for POF Bragg gratings is greater than that for SOF Bragg gratings

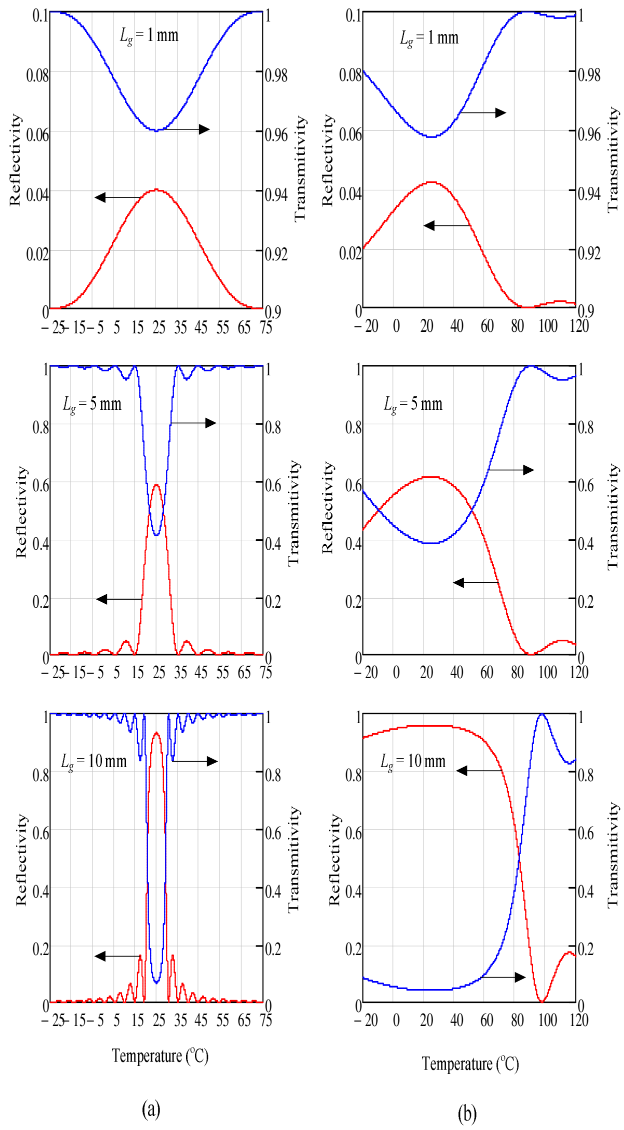

Figure 6 Reflection (red curves) and transmission (blue curves) spectral response verses temperature variation with Δ_n = $1{\times}10^{-4}$ (a) SOF Bragg gratings, and (b) POF Bragg gratings, respectively

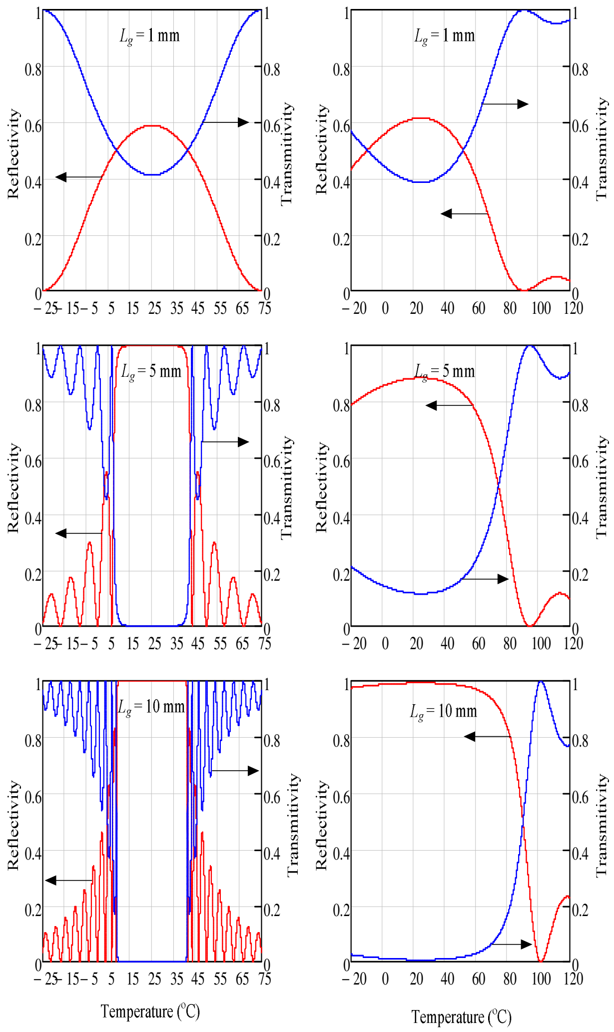

(a) (b)

Figure 7 Reflection (red curves) and transmission (blue curves) spectral response verses temperature variation with $\Delta_n = 5\times10^{-4}$ for (a) SOF Bragg gratings and (b) POF Bragg gratings

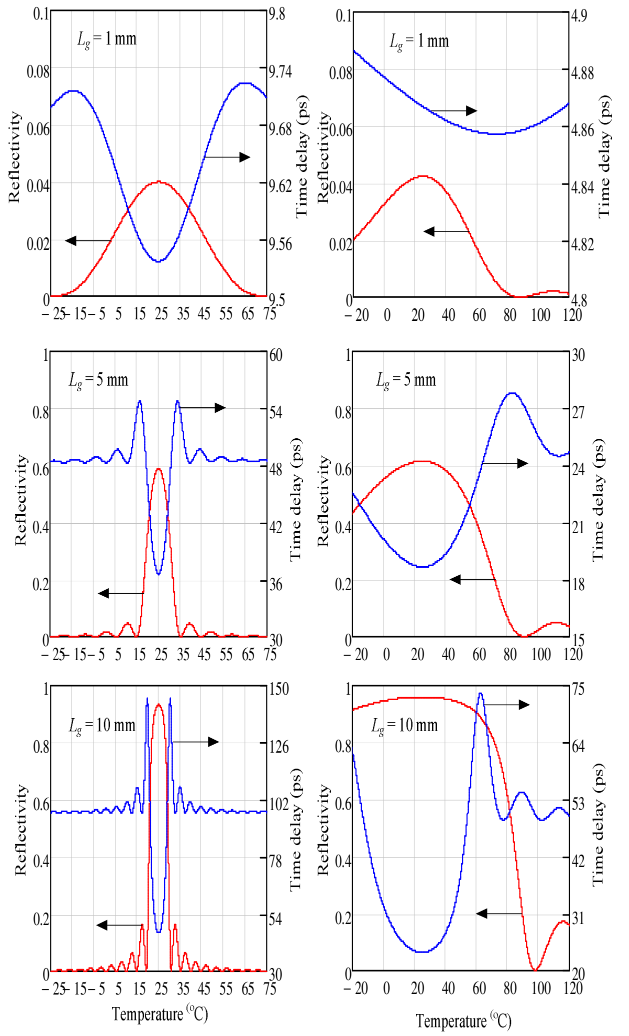

(a) (b)

Figure 8 Reflection (red curves) and time delay (blue curves) spectral response versus temperature variation with $\Delta n = 1\times10^{-4}$ for (a) SOF, Bragg gratings and (b) POF Bragg gratings

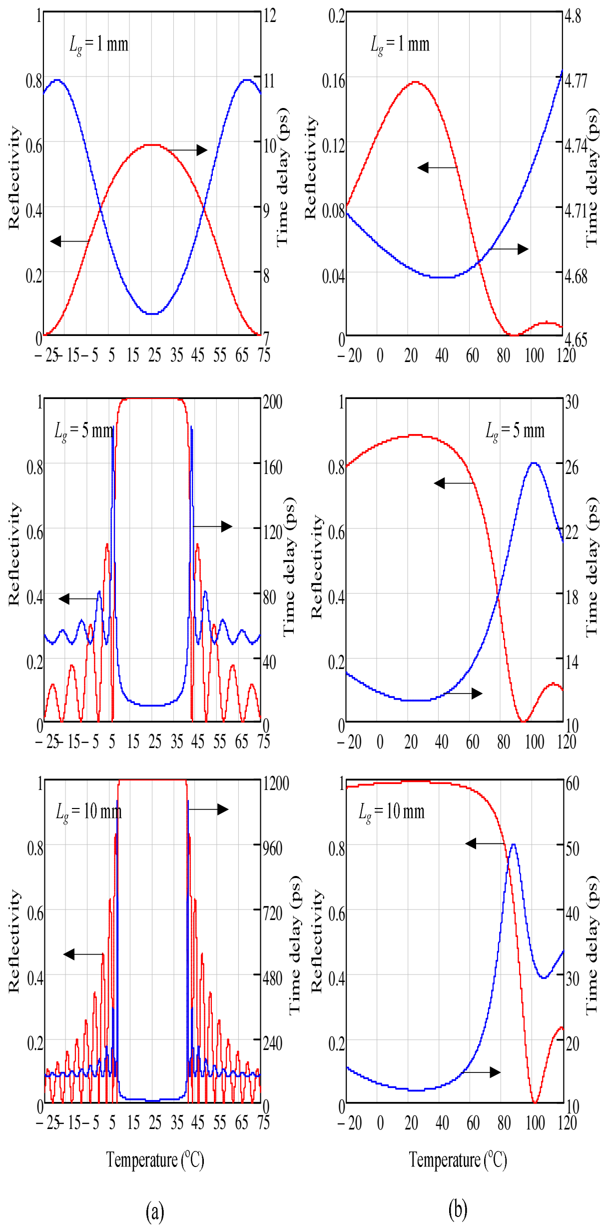

Figure 9 Reflection (red curves) and time delay (blue curves) spectral response versus temperature variation with Δn = 5×10^{-4} for (a) SOF Bragg gratings and (b) POF Bragg gratings

V. CONCLUSION

The present work constitutes the first study on temperature effect on the polymer optical fiber (POF) Bragg gratings spectral response. Due to the unique large and negative temperature coefficient of the POF Bragg gratings, the spectral response showed high stability with temperature change compare with that for silica optical fiber (SOF) Bragg gratings. For example, with kL_g = 1, the reflectivity of SOF Bragg gratings is decreases significantly from 58% to 0.05% by changing temperature ΔT = 10 °C (from 25 to 35 °C). In contrast, by changing temperature ΔT = 50 °C (from 25 to 75 °C), the reflectivity of POF Bragg gratings decrease from 60% to 15%. With the increase of the kL_g to 3, by increasing temperature from 25 to 35 °C, the SOF Bragg gratings reflectivity reduces from 99% to 6.5% comparing with the reduction in the POF Bragg gratings reflectivity from 99% to 89% by changing temperature from 25 to 75 °C. Results show that, by increasing kL_g, the peak reflectance value increases; the bandwidth of the Bragg reflector become narrower and τ_r deceasing significantly and reach its minimum value at the designed wavelength (λ_B). Also, the peak reflectivity value increases to around 60% when the Δ_n value increases from 1×10^{-4} to 5×10^{-4}.

REFERENCES

[1] D. Heo, D. -J. Shin, I. -K. Yun, J. -S. Lee, J. Jeong, J. Lee, "BLS polarization-induced performance degradation in WDM–PON systems based on wavelength-locked FP-LDs," *Opt. Commun,*. vol. 283, pp. 258–261, 2010.

[2] M. Li, W. Hong, X. Zhang, W. Li, D. Huang, "Investigation of a high-speed optical FSK scheme for WDM-PON applications with centralized lightwave source," *Opt. Commun, vol.* 283, pp. 1251–1260, 2010.

[3] F. Y. Shih, C. H. Yeh, C. W. Chow, C. H. Wang, S. Chi, “Utilization of self-injection Fabry–Perot laser diode for long-reach WDM-PON,” *Optical Fiber Technology*, vol.16, pp. 46–49, 2010.

[4] L. S. Yan, A. Yi, W. Pan, B. Luo, “A Simple Demodulation Method for FBG Temperature Sensors Using a Narrow Band Wavelength Tunable DFB Laser,” *IEEE photon Tech. Lett.*, vol. 22, pp. 1391- 1393, 2010.

[5] R. A. Vazquez-Sanchez, E. A. Kuzin, C. M. Garca-Lara, M. May-Alarcon, J. L. Camas-Anzueto, G. C. Righini, S. V. Miridonov, “Radio-frequency interrogation of a fiber Bragg grating sensor in the configuration of a fiber laser with external cavities,” *Optik*, vol. 121, pp. 2040–2043, 2010.

[6]F. N. Timofeev, , G. Simin, M. Shatalov, S. Gurevich, P. Bayvel, R. Wyatt , I. Lealman, R. Kashyap, “Experimental and theoretical study of high temperature-stability and low-chirp 1.55 micron semiconductor laser with an external fiber grating,” *Fiber Integr. Opt.*, vol. 19, pp. 327–354, 2000.

[7]J. –R. Lee, S. Y. Chong, C. –Y. Yun, D. –J. Yoon, “A lasing wavelength stabilized simultaneous multipoint acoustic sensing system using pressure-coupled fiber Bragg gratings,” *Optics and Lasers in Engineering*, vol. 49, pp. 110–120, 2011.

[8]Z. C. Zhuo, B. S. Ham, “A temperature-insensitive strain sensor using a fiber Bragg grating,” *Opt. Fiber Technol.*, vol 15, pp. 442–444, 2009.

[9]H. Liu, H. Liu, G. Peng, T. W. Whitbread, “Tunable dispersion using linearly chirped polymer optical fiber Bragg gratings with fixed center wavelength,” *IEEE photon Tech. Lett.*, vol. 17, pp. 411–413, 2005.

[10]H. Y. Liu, H. B. Liu, G. D. Peng, P. L. Chu, “Polymer optical fiber Bragg gratings based fiber laser,” *Opt. Commun.*, vol. 266, pp. 132–135, 2006.

[11]H. Y. Liu, H. B. Liu, G. D. Peng, “Tensile strain characterization of polymer optical fiber Bragg gratings,” *Opt. Commun.*, vol. 251, pp. 37–43, 2005.

[12]A. Othonos, K. Kalli, “Fiber Bragg Grating-Fundamentals and Applications in Telecommunications and Sensing,” Artech House, Boston, 1999.

[13]L. Eldada, L. W. Shacklette, “Advances in polymer integrated optics,” *IEEE J. Sel. Top. Quantum Electron.*, vol. 6, pp. 54–68, 2000.

[14]H. Y. Liu, G. D. Peng, P. L. Chu, “Thermal stability of gratings in PMMA and CYTOP polymer fibers,” *Opt. Commun.*, vol. 204, pp. 151–156, 2002.

[15]G. Jeong, J. –H. Lee, M. Y. Park, C. Y. Kim, S. –H. Che, W. Lee, B. W. Kim, “Over 26-nm wavelength tunable external cavity laser based on polymer waveguide platforms for WDM access networks,” *IEEE photon Tech. Lett.*, vol. 18, pp. 2102–2104, 2006.

[16]Y. –O. Noh, H. –J. Lee, J. J. Ju, M. –S. Kim, S. H. Oh, M. –C. Oh, “Continuously tunable compact lasers based on thermo-optic polymer waveguides with Bragg gratings,” *Opt. Express*, vol. 16, pp. 18194–18201, 2008.

[17]W. Yuan, A. Stefani, M. Bache, T. Jacobsen, B. Rose, N. Herhold-Rasmussen, F. K. Nielsen, S. Andresen, O. B. Sorensen, K. S. Hansen, O. Bang, “Improved thermal and strain performance of annealed polymer optical fiber Bragg gratings,” *Opt. Commun.,* vol. 284, pp. 176–182, 2011.

[18]T. Erdogan, “Fiber grating spectra,” *J. Lightwave Technol.*, vol. 15, pp. 1277–1294, 1997.